Technische Mechanik, Band 14, Heft 2, (1994), 147-154
Manuskripteingang 08. Juni 1994

Numerical Calculation of Steady Meniscus of Liquid in a Slow Spin Container under a Micro Gravity Field

G. W. Bao

A liquid partially filling a slow spin container forms its free surface in a meniscus shape due to microgravity, small centrifugal and strong capillary force conditions. Such a meniscus is governed by an ordinary differential equation where two parameters and one boundary are indefinite and may be determined by iteration. Conventional iteration adopted in solving this problem is called „simple shooting method", but it was found that using this method the divergence degree is strong. A bilateral shooting method is suggested in the present paper and the numerical tests show that the convergence is comparatively good.

Introduction

In order to study the sloshing of a liquid in a slowly spinning container under microgravity conditions (Concus et al, 1969; Chu, 1970; Schilling and Siekmann, 1991; Ebert, 1984; Bao, 1989; Bauer and Eidel, 1991), we should firstly determine the configuration of the free surface of the steady-spin fluid (Concus et al, 1969; Ebert, 1984; Bauer and Eidel, 1991; Hastings and Rutherford, 1969; Salzman, 1970; Utsumi and Kondo, 1987). In this case, the free surface forms a meniscus due to the effect of a strong capillary force. Such a meniscus is governed by an ordinary differential equation where there are two indefinite parameters and one indefinite boundary for spheroidal cavities. Generally speaking, these unknown variables can be determined by iteration. Conventional iteration adopted in solving this problem is called „simple shooting method" (Concus et al, 1969; Utsumi and Kondo, 1987). But when employing this technique, we have found that the choice of an initial value for iteration is difficult. Numerical experiments show that when the chosen initial value is very close to the target value, the iteration is convergent; but when the chosen initial value is not close enough to the target value, the iteration will diverge in integrating the ordinary differential equation based on the shooting variables in the iterative procedure, and thus the computer program will stop integrating and exit running.

To overcome the above divergence, a bilateral shooting method is suggested here. Using this method, numerical tests show that the convergence is enhanced compared to the conventional shooting method. That is, we can enlarge the convergent neighborhood of the target point and thus keep the iteration process moving.

Equation and Boundary Conditions

Assume that the container is spheroidal and rotates slowly around its symmetric axis at a spin rate ω_0. The steady-state motion of the contained liquid is assumed to rotate around the coaxis with ω_0 in rigid model. A tank fixed cylindrical coordinate system (r, φ, z) is introduced with origin at the container center and the z-axis coaxial to the spin axis.
Under micro-gravity conditions, the effect of liquid surface tension is remarkable and cannot be neglected. Thus, the governing equation for the meniscus can be derived from Bernoulli's first integral,

$$gz - \frac{1}{2}\omega_0^2 r^2 + \frac{p}{\rho} = \text{constant}$$

and Laplace-Young formula for surface tension,

$$p_u - p = \sigma\kappa$$

in dimensionless from

$$B_g Z - \frac{1}{2} B_\Omega R^2 - \kappa = B_g Z_0 - 2\kappa_0 \tag{1}$$

for the case that the bottom of the free surface is on the spin axis. In equation (1), $B_g = \rho g a^2 / \sigma$ and $B_\Omega = \rho \omega_0^2 a^3 / \sigma$ are respective Bond numbers for micro-gravity g and slow ω_0. The quantity κ is the mean curvature and κ_0 is the curvature at the bottom of the meniscus curve on the meridian plane $(\varphi = \text{constant})$. Introducing $y(\vartheta)$, $0 = \vartheta_1 \le \vartheta \le \vartheta_2$, to represent the meniscus (Figure 1) with the origin c on the z-axis, then we have

$$\begin{cases} R = y(\vartheta)\sin\vartheta \\ Z = Z_c - y(\vartheta)\cos\vartheta \end{cases} \tag{2}$$

and the expression of the mean curvature can thus be derived.

$$\kappa = \frac{\left(2y_\vartheta^2 - yy_{\vartheta\vartheta} + y^2\right)}{\left(y^2 + y_\vartheta^2\right)^{3/2}} + \frac{\left(1 - \frac{y_\vartheta}{y}\cot\vartheta\right)}{\left(y^2 + y_\vartheta^2\right)^{1/2}} \tag{3}$$

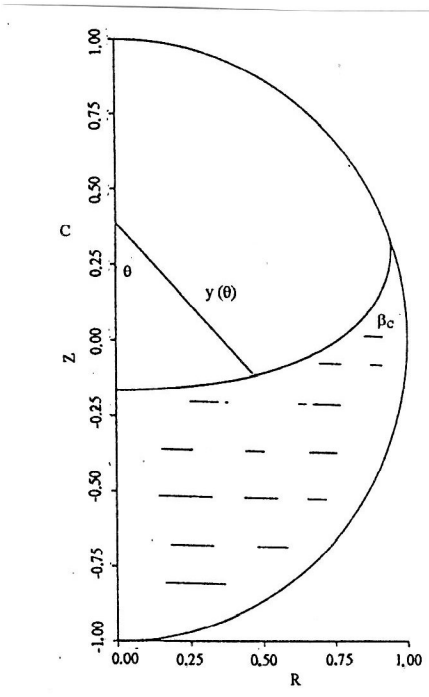

Figure 1. Coordinate systems

Substituting expressions (2) and (3) into equation (1), one obtains the governing equation.

$$y_{\vartheta\vartheta} = \left(2y_{\vartheta}^2 + y^2\right)\frac{1}{y} + \left(1 - \frac{y_{\vartheta}}{y}\cot\vartheta\right)\frac{\left(y^2 + y_{\vartheta}^2\right)}{y}$$
$$- \left[B_g\left(Z_c - Z_0 - y\cos\vartheta\right) - \frac{1}{2}B_{\Omega}y^2\sin^2\vartheta + 2\kappa_0\right]\frac{\left(y^2 + y_{\vartheta}^2\right)^{3/2}}{y} \tag{4}$$

$$0 \le \vartheta \le \vartheta_2$$

Due to symmetry, the boundary conditions at $\vartheta = 0$ are

$$\begin{cases} y(0) = Z_c - Z_0 \\ y_{\vartheta}(0) = 0 \end{cases} \tag{5}$$

The container wall is represented by

$$\begin{cases} R = \sin\alpha \\ Z = -\dfrac{b}{a}\cos\alpha \end{cases}$$

Let α_2 be the parameter denoting the contact point, then one gets the expressions of ϑ_2 and $y\left(\vartheta_2\right)$ with respect to α_2.

$$\begin{cases} \vartheta_2 = \tan^{-1}\left(\dfrac{\sin\alpha_2}{Z_c + \dfrac{b}{a}\cos\alpha_2}\right) \\ y\left(\vartheta_2\right) = \left[\sin^2\alpha_2 + \left(Z_c + \dfrac{b}{a}\cos\alpha_2\right)^2\right]^{1/2} \end{cases} \tag{6}$$

For a given contact angle β_c, the boundary condition y_{ϑ} at $\vartheta = \vartheta_2$ is obtained.

$$y_{\vartheta}\left(\vartheta_2\right) = y\left(\vartheta_2\right)\frac{\cos\alpha_2\sin\left(\vartheta_2 + \beta_c\right) - \dfrac{b}{a}\sin\alpha_2\cos\left(\vartheta_2 + \beta_c\right)}{\cos\alpha_2\cos\left(\vartheta_2 + \beta_c\right) + \dfrac{b}{a}\sin\alpha_2\sin\left(\vartheta_2 + \beta_c\right)} \tag{7}$$

Bilateral Shooting Technique

For a given filling ratio γ and contact angle β_c and a fixed Z_c equation (4) and boundary conditions (5), (6) and (7) show that parameters Z_0, κ_0 and α_2 are indefinite and can be determined by the following bilaterial shooting method.

Set two initial value problems as follows:

$$\begin{cases} y_{\vartheta\vartheta} = \left(2y_{\vartheta}^2 + y^2\right)\dfrac{1}{y} + \left(1 - \dfrac{y_{\vartheta}}{y}\cot\vartheta\right)\dfrac{\left(y^2 + y_{\vartheta}^2\right)}{y} \\ \qquad - \left[B_g\left(Z_c - Z_0 - y\cos\vartheta\right) - \dfrac{1}{2}B_{\Omega}y^2\sin^2\vartheta + 2\kappa_0\right]\dfrac{\left(y^2 + y_{\vartheta}^2\right)^{3/2}}{y} \\ \qquad\qquad\qquad\qquad\qquad\qquad 0 \le \vartheta \le \vartheta_t \\ y\ (0) = Z_c - Z_0 \\ y_{\vartheta}(0) = 0 \end{cases} \tag{8}$$

$$\begin{cases} y_{\vartheta\vartheta} = \left(2y_{\vartheta}^2 + y^2\right)\dfrac{1}{y} + \left(1 - \dfrac{y_{\vartheta}}{y}\cot\vartheta\right)\dfrac{\left(y^2 + y_{\vartheta}^2\right)}{y} \\ \qquad - \left[B_g\left(Z_c - Z_0 - y\cos\vartheta\right) - \dfrac{1}{2}B_{\Omega}y^2\sin^2\vartheta + 2\kappa_0\right]\dfrac{\left(y^2 + y_{\vartheta}^2\right)^{3/2}}{y} \\ \qquad\qquad\qquad\qquad\qquad\qquad \vartheta_t \le \vartheta \le \vartheta_2 \\ y\left(\vartheta_2\right) = \left[\sin^2\alpha_2 + \left(Z_c + \dfrac{b}{a}\cos\alpha_2\right)^2\right]^{1/2} \\ y_{\vartheta}\left(\vartheta_2\right) = y\left(\vartheta_2\right)\dfrac{\cos\alpha_2\sin\left(\vartheta_2 + \beta_c\right) - \dfrac{b}{a}\sin\alpha_2\left(\vartheta_2 + \beta_c\right)}{\cos\alpha_2\cos\left(\vartheta_2 + \beta_c\right) + \dfrac{b}{a}\sin\alpha_2\sin\left(\vartheta_2 + \beta_c\right)} \end{cases} \tag{9}$$

and integrate the initial value problem (8) from one side and the initial value problem (9) from the other side, represented by y^+ and y^- respectively. Then the target equations are

$$\begin{cases} y^+\left(\vartheta_t;\ Z_0,\ \kappa_0\right) - y^-\left(\vartheta_t;\ Z_0,\ \kappa_0,\ \alpha_z\right) = 0 \\ y_{\vartheta}^+\left(\vartheta_t;\ Z_0,\ \kappa_0\right) - y_{\vartheta}^-\left(\vartheta_t;\ Z_0,\ \kappa_0,\ \alpha_2\right) = 0 \\ \gamma - \dfrac{V_{\text{fluid}}\left(Z_0, \kappa_0\alpha_2\right)}{V_{\text{tank}}} = 0 \end{cases} \tag{10}$$

which indicate that Z_0, κ_0, α_2 can be determined by iteration.

Choice of Initial Value for Iteration

The choice of initial value for iteration is simple. If we have got the target value $v_0 = \left(Z_0,\ \kappa_0,\ \alpha_2\right)_0$ in a given parameter state $u_0 = \left(B_g,\ B_{\Omega},\ \gamma,\ \beta_c\right)$ and we want to calculate $v_{\mathbf{T}} = \left(Z_{\mathbf{0}}, \kappa_{\mathbf{0}}, \alpha_{\mathbf{z}}\right)_{\mathbf{T}}$ in a terminal parameter

state $u_T = \left(B_g, B_\Omega, \gamma, \beta_c\right)_T$, the initial value $v_T^{(0)}$ can be obtained through an n-step calculation. We introduce n parameter states $u_i(i = 1,\ldots,n)$ such that

$$u_i = u_0 \frac{n-i}{n} + u_T \frac{i}{n} \qquad i = 1,\ldots n$$

and then take target value v_i as initial value for iteration in the $i+1^{th}$ state u_{i+1}, i.e., $v_{i+1}^{(0)} = v_i$ step by step from $i =$ to $i = n - 1$. Finally we get a suitable initial value $v_T^{(0)}(= v_{n-1})$ and then the target value v_T can be determined.

Numerical Results

Table 1 to Table 5 present the computational results of ν in various parameter conditions. The initial value for iteration in each row presented in the tables is taken from target value in the neighboring row. It will diverge in such step-lengths if we employ the simple shooting method. The nodal coefficient τ in the tables denotes that $\tau = \vartheta_t / \vartheta_z$.

Figure 2 to Figure 6 are configurations of meniscus correspond to Table 1 to Table 5, respectively.

β_c (deg)	Z_0	κ_0	α_2 (deg)
0.	-.1641	0.3717	111.60
5.	-.1635	0.3709	110.36
10.	-.1615	0.3683	109.11
20.	-.1539	0.3569	106.61
30.	-.1415	0.3357	104.12
40.	-.1247	0.3037	101.66
50.	-.1043	0.2604	99.26
60.	-.0808	0.2064	96.89
70.	-.0551	0.1433	94.56
80.	-.0279	0.0734	92.27
90.	0.0000	0.0000	90.00
100.	0.0279	-.0734	87.73
110.	0.0551	-.1433	85.44
120.	0.0808	-.2064	83.11
130.	0.1043	-.2604	80.75
140.	0.1247	-.3037	78.34
150	0.1415	-.3357	75.88
160.	0.1539	-.3569	73.39
170.	0.1616	-.3683	70.89
175.	0.1635	-.3709	69.64
180.	0.1641	-.3717	68.40
$b/a = 1, B_g = 10, B_\Omega = 0, \gamma = .5, \tau = .9$			

Table 1. Target values versus contact angle

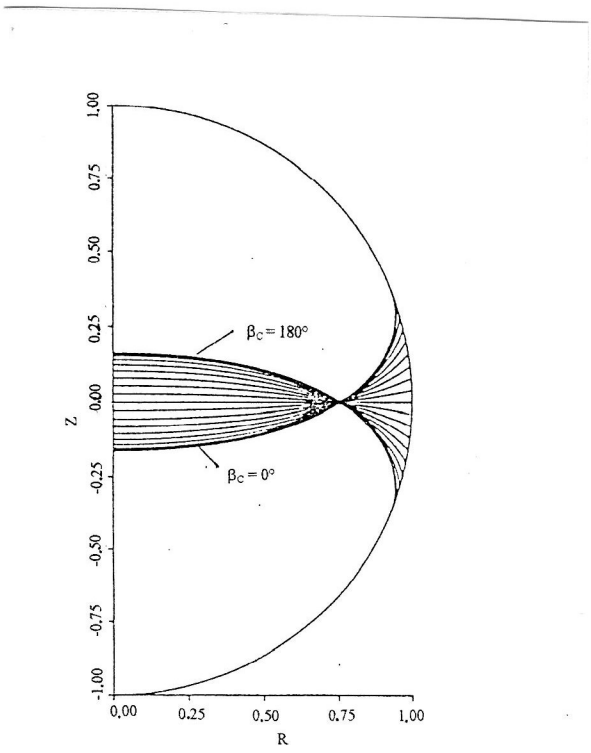

Figure 2. Meniscus versus contact angle

B_g	Z_0	κ_0	α_2 (deg)
0.	-.5738	1.2595	161.69
1.	-.3971	1.0539	131.84
3.	-.2912	0.7958	120.92
5.	-.2367	0.6251	116.18
10.	-.1635	0.3709	110.36
20.	-.0998	0.1560	105.39
30.	-.0706	0.0748	102.92
40.	-.0540	0.0390	101.37
50.	-.0435	0.0215	100.27
60.	-.0363	0.0124	99.44
70	-.0311	0.0074	98.79
80.	-.0271	0.0045	98.26
90.	-.0240	0.0028	97.81
100.	-.0216	0.0018	97.43
110.	-.0196	0.0012	97.10
120.	-.0179	0.0007	96.81
$b/a = 1, \beta_c = 5°, B_\Omega = 0, \gamma = .5, \tau = .9$			

Table 2. Target values versus gravity Bond number

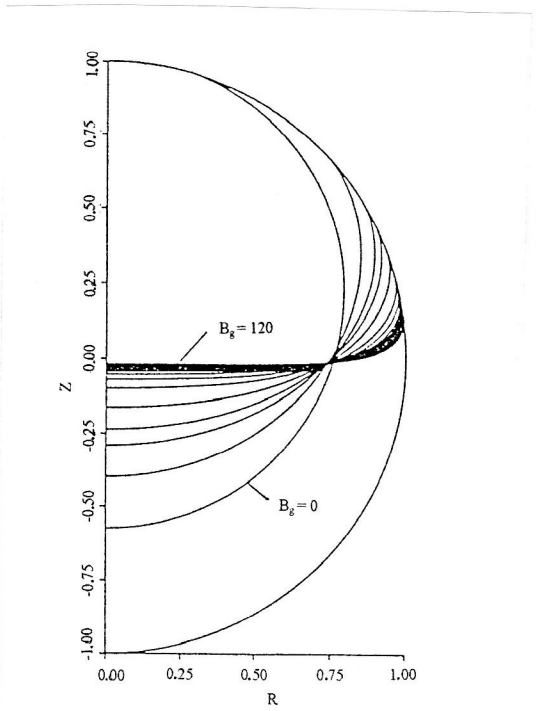

Figure 3. Meniscus versus gravity Bond number

τ	B_Ω	Z_0	κ_0	α_2 (deg)
	0.	-.1635	0.3709	110.36
	1.	-.1767	0.4322	111.05
	3.	-.2033	0.5525	112.42
.9	5.	-.2300	0.6693	113.79
	7.	-.2567	0.7824	115.14
	9.	-.2835	0.8918	116.47
	10.	-.2970	0.9451	117.13
	12.	-.3238	1.0487	118.41
	14.	-.3506	1.1484	119.64
.8	16.	-.3774	1.2445	120.83
	18.	-.4041	1.3368	121.97
	20.	-.4306	1.4256	123.05
	22.	-.4570	1.5111	124.07
	24.	-.4833	1.5933	125.05
.7	26.	-.5094	1.6725	125.97
	28.	-.5353	1.7488	126.84
	30.	-.5609	1.8224	127.67
	32.	-.5864	1.8934	128.45
$b/a = 1,\ B_g = 10, \beta_c = 5°, \gamma = .5$				

Table 3. Target values versus spin Bond number

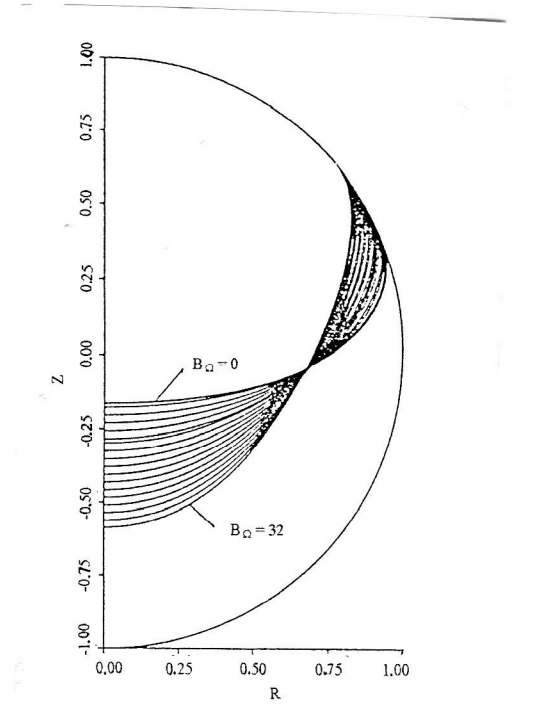

Figure 4. Meniscus versus spin Bond number

γ	Z_0	κ_0	α_2 (deg)
.0010	-.9793	0.6569	21.51
.0050	-.9511	0.5999	33.22
.0100	-.9264	0.5490	39.36
.0500	-.8040	0.4094	57.61
.1000	-.7000	0.3553	68.29
.2000	-.5389	0.3196	82.07
.3000	-.4037	0.3176	92.51
.4000	-.2807	0.3348	101.67
.5000	-.1635	0.3709	110.36
.6000	-.0480	0.4325	119.07
.7000	0.0699	0.5370	128.29
.8000	0.1965	0.7315	138.70
.9000	0.3496	1.1953	151.87
.9500	0.4593	1.8289	161.01
.9800	0.5715	2.9389	168.90
.9900	0.6417	4.0104	172.68
.9950	0.7026	5.3243	175.20
.9990	0.8130	9.6764	178.21
$b/a = 1, B_g = 10, B_\Omega = 0, \beta_c = 5°, \tau = .9$			

Table 4. Target values versus filling ratio - spherical tank

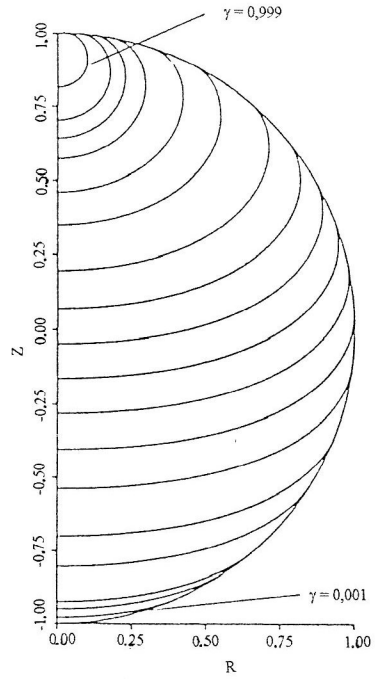

Figure 5. Meniscus versus filling ratio - spheroidal tank

γ	Z_0	κ_0	α_2
.0100	-.6693	0.4210	39.89
.0500	-.5908	0.3478	61.92
.1000	-.5250	0.3223	75.24
.2000	-.4248	0.3172	91.82
.3000	-.3416	0.3366	103.27
.4000	-.2661	0.3738	112.59
.5000	-.1940	0.4317	120.96
.6000	-.1225	0.5197	129.02
.7000	-.0482	0.6596	137.27
.8000	0.0347	0.9060	146.31
.9000	0.1437	1.4601	157.37
.9500	0.2312	2.1828	164.84
.9800	0.3289	3.4170	171.16
.9900	0.3928	4.5987	174.17
.9950	0.4490	6.0475	176.17
.9990	0.5508	10.8653	178.55
$b/a = .72, B_g = 10, B_\Omega = 0, \beta_c = 5°, \tau = .9$			

Table 5. Target values versus filling ratio - spheroidal tank

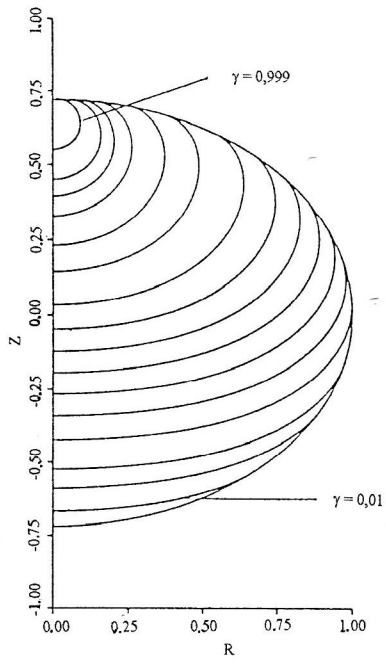

Figure 6. Meniscus versus filling ratio - spheroidal tank

Acknowledgement

This research was sponsored by the Chinese National Natural Science Foundation.

Literature

1. Bao, G.W.: Liquid Sloshing in a Slow Spinning Container under Low Gravity Environment, Proc. of ASIA Vib. Conf. '89, (Wen, B.C.; Zheng, Z.C. ed.), Press of Northeast Univ. of Technology, Shengyang, China, (1989), 730-734.

2. Bauer, H.F.; Eidel, W.: Vibrations of a Cylindrical Liquid Column under the Influence of a Steady Axial Micro-Gravity Field, Microgravity Sci. Technology, 3, 4, (1991), 238-245.

3. Chu, W.H.: Low-Gravity Fuel Sloshing in an Arbitrary Axisymmetric Rigid Tank, Trans. ASME, J. Appl. Mech., 37, (1970), 828-837.

4. Concus, P.; et al: Small Amplitude Lateral Sloshing in Spheroidal Containers under Low Gravitational Conditions, NASA-LeRC, CR-72500, LMSCA944673, NAS3-9704, (1969).

5. Ebert, K.: Fluid Slosh Studies, vol. 2 - Study of Slosh Dynamics of Fluid Filled Containers on Slowly Rotating Spacecraft, NASA N86-14550, ESA-CR(P)-2077-vol-2, (1984).

6. Hastings, L.J.; Rutherford III, R.: Low Gravity Liquid-Vapor Interface Shapes in Axisymmetric Containers and a Computer Solution, NASA-MSFC, TM X-53790, (1969).

7. Salzman, J.A.: Low-Gravity Liquid-Vapor Interface Configurations in Spheroidal Containers, NASA-LeRC, TN D-5648, (1970).

8. Schilling, U.; Siekmann, J.: Numerical Calculation of the Natural Frequencies of a Sloshing Liquid in Axial Symmetrical Tanks under Strong Capillary and Weak Gravity Conditions, Isr. J. of Technol., 19, (1981), 44-50.

9. Utsumi, M.; Kondo, H.: Liquid Sloshing in a Spherical Container at Low-Gravity Environments (1st Report, Static Configuration of Liquid Surface) (in Japanese), Trans JSME C, 53, 492, (1987), 1683-1690.

Address: Dr. G.W. Bao, Associate Professor, Department of Engineering Mechanics, Shanghai Jiao Tong University, 1954 Hua Shan Lu, Shanghai 200030, People's Republic of China